



Contents lists available at ScienceDirect

## The Saudi Dental Journal

journal homepage: [www.ksu.edu.sa](http://www.ksu.edu.sa)  
[www.sciencedirect.com](http://www.sciencedirect.com)

Original Article

## Comparative evaluation of bioactivity of MTA plus and MTA plus chitosan conjugate in phosphate buffer saline an invitro study

Geeta Hiremath<sup>a,\*</sup>, Shreshtha Pramanik<sup>a</sup>, Priya Horatti<sup>a</sup>, Anil<sup>b</sup><sup>a</sup> Dept. Conservative Dentistry and Endodontics, SDM College of Dental Sciences and Hospital, Dharwad, Karnataka, India<sup>b</sup> Dept. Biochemistry, SDM College of Medical Sciences and Hospital, Dharwad, India

## ARTICLE INFO

## Keywords:

Apatite  
Bioactivity  
Chitosan  
Mineral Trioxide Aggregate Plus  
Scanning electron microscope

## ABSTRACT

**Background and Objective:** Various materials like MTA, Biodentine etc have been used for the regeneration of lost dental tissues. Still, the quest for newer materials to enhance the bioactivity of the existing materials continues. Hence this study aims at the evaluation of bioactivity of MTA Plus when conjugated with Chitosan in phosphate buffer saline.

**Methodology:** Materials used were MTA Plus (Group 1), MTA Plus and chitosan conjugate (Group 2). The materials were mixed and placed in phosphate buffer saline. Bioactivity of Group 1 and Group 2 materials were assessed at 7 days and 28 days time intervals using SEM-EDX analysis.

**Results:** SEM analysis of group 1 revealed a compact and agglomerate lath-like appearance with uniform particle size. SEM analysis of group 2 reveals acicular and lath-like appearance of the precipitate on the material surface. EDX analysis of the freshly prepared materials gave the qualitative semiquantitative elemental composition on the material surfaces after immersion in PBS for 7 and 28 days.

**Conclusion:** MTA Plus Chitosan conjugate had greater potential to form apatite crystals on its surface. Hence, Chitosan can be used as a vehicle for the currently available materials to enhance the bioactivity and fasten the healing process.

## 1. Introduction

Dental materials have undergone a significant evolution in recent years. Inert materials are now used for reconstruction rather than replacing the lost tissue. This reconstruction is possible only by the combined effect of newer techniques and the bioactive materials (Primozic et al., 2022). Bioactive in restorative dentistry, usually refers to the ability of a material to form hydroxyapatite crystals on its surface. However, from a biological perspective, the materials that potentially interact in a positive way with living cells and tissues are called as bioactive material (Vallittu et al., 2018).

In Endodontics, Calcium hydroxide was one of the first materials with bioactive characteristics. The cement was used to promote the formation of a dentinal bridge on exposed pulp tissue (Tiskaya et al., 2021). In the recent years, mineral trioxide aggregate (MTA) and modified MTA like MTA Plus have been developed. The bioactivity of these calcium silicate materials is a result of their potential to induce the formation of hydroxyapatite crystals on their surface (Walsh et al., 2018). Another material which has gained popularity as vehicle in

medical field is Chitosan. Chitosan is natural biodegradable polymer produced by deacetylation of chitin. It is derived from the exoskeleton of insects, crustaceans and cell walls of some fungi such as *Aspergillus* and *Mucor* (<https://www.epj-conferences.org>). Chitosan is an ideal material for biomedical applications because of its distinctive biological properties like good biodegradability, biocompatibility, osteoconductivity and anti-microbial properties. It is also a material for hard tissue repair (Ahmadi et al., 2015).

Chitosan as a vehicle has been widely discussed in research paper due to its property to coat and protect the molecules of dental materials from degradation. It also controls the rate of release of ions. It serves as a semi-synthetic extracellular matrix to provide an amenable environment for cellular adherence and re-modelling (Fenice and Gorrasi, 2021). Recently, Ruan et al. employed a Chitosan-based hydrogel as a delivery medium for amelogenin with the aim of regenerating the aligned crystal structure. The use of Chitosan offers a dual effect of protection against secondary caries owing to its antibacterial properties without influencing the enamel crystal orientation (Ruan and Moradian-Oldak, 2015). Studies must be performed especially on human cells, to ensure

\* Corresponding author.

E-mail addresses: [geethahiremath7@yahoo.co.in](mailto:geethahiremath7@yahoo.co.in) (G. Hiremath), [shreshtha\\_pnik20222@yahoo.com](mailto:shreshtha_pnik20222@yahoo.com) (S. Pramanik), [anymh9832@rediffmail.com](mailto:anymh9832@rediffmail.com) (Anil).<https://doi.org/10.1016/j.sdentj.2024.05.008>

Received 16 November 2023; Received in revised form 14 May 2024; Accepted 19 May 2024

Available online 23 May 2024

1013-9052/© 2024 THE AUTHORS. Published by Elsevier B.V. on behalf of King Saud University. This is an open access article under the CC BY-NC-ND license (<http://creativecommons.org/licenses/by-nc-nd/4.0/>).

that these new materials are biocompatible when in close contact with living tissues. The compounds in them may either interfere in the healing process or can repair the damaged tissue. The incorporation of various particles into each other can not only improve their physico-chemical properties but also the biocompatibility, pH, sealing ability and calcium releasing ability (Tu et al., 2018). A study conducted to

characterize the compatibility of chitosan as a biomaterial along with MTA plus using FTIR, AFM, concluded that the material conjugates well and chitosan can be used as a vehicle for biomaterials (Hiremath et al., 2020a). With this respect, various studies have shown the conjugation of two materials and their synergistic activity. Some of the studies conducted on the incorporation of chitosan in composite scaffold have

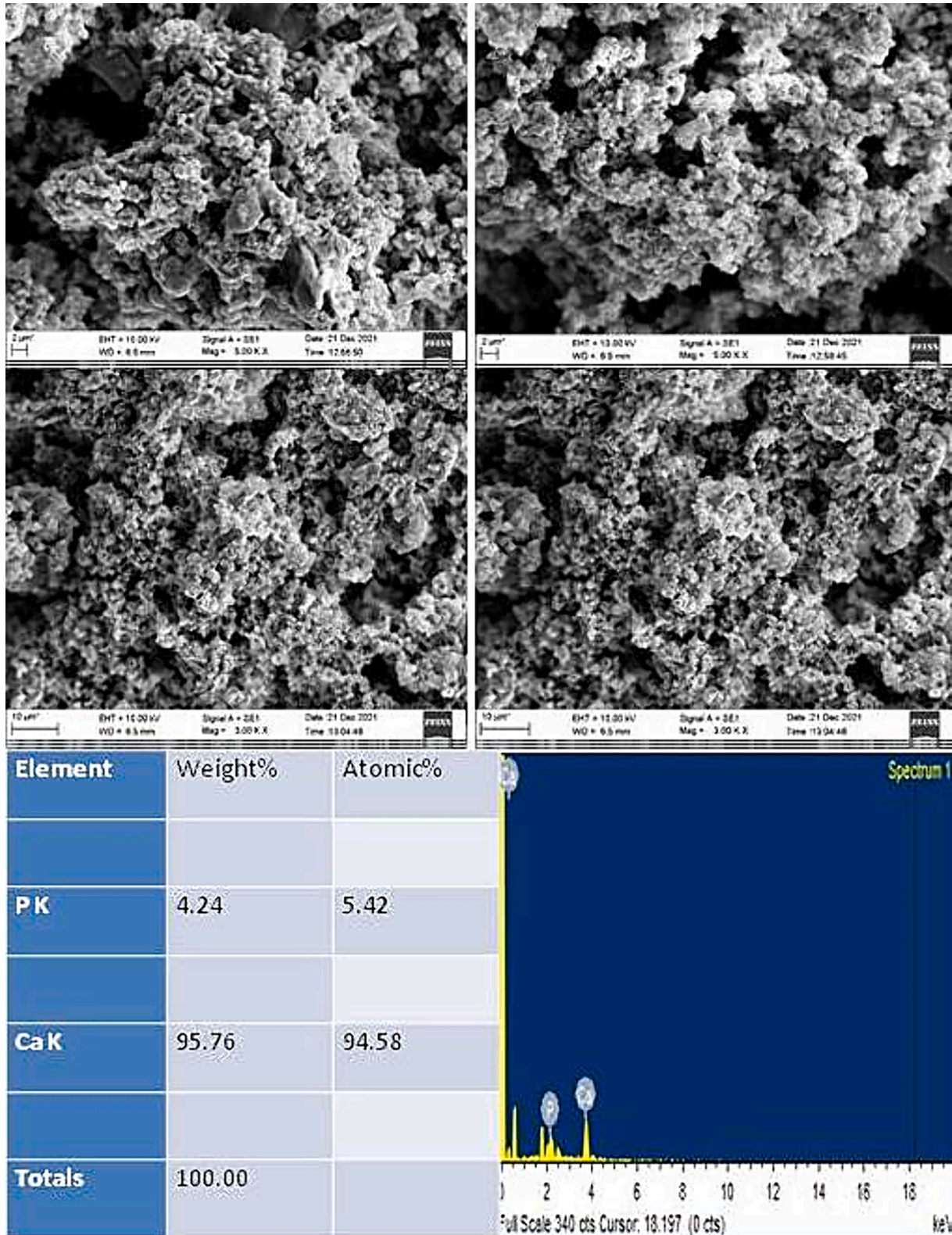


Fig. 1. SEM image and EDX analysis of Group 1 after 7 days.

shown promising bioactivity on dental pulp stem cells (Gurucharan et al., 2023). The antibiofilm activity of MTA Plus and chitosan conjugate (Singh et al., 2020), and their effect on cell viability of Periodontal ligament cells (Hiremath et al., 2020b) have been studied. But there are no studies of these materials on the bioactivity. The surface morphology of the material surface aids in assessing the bioactivity of the material.

Thus, this study aims to evaluate the surface morphology of the materials when in contact with Phosphate buffer saline. This study helps us in knowing the bioactivity of the materials.

## 2. Material and Methods

The purpose of this study was to evaluate and compare the bioactivity of MTA plus and MTA Plus – Chitosan Conjugate in Phosphate Buffer Saline. The study protocol was approved by the Institutional Review Board and Ethical Committee of the Institution.

### 2.1. Sample Preparation

MTA Plus powder was mixed with its gel as recommended by the manufacturers for group 1.

For conjugate (group 2) MTA Plus was mixed with 2 % Chitosan gel (Mol.wt 350 Kda, Deacetylation > 75 % (SigmaAldrich – Cat No. 101700976). Due to high acetylation rate, Chitosan was dissolved in 2 % acetic acid in water. The materials were grouped as follows.

GROUP 1– MTA Plus mixed with the proprietary gel

GROUP 2- MTA Plus mixed with 2 % Chitosan gel

Freshly mixed sample from group 1 and 2 was immersed vertically in centrifuge tubes containing 15 ml PBS (HI-Media). The tubes were stored at 37 °C and PBS was renewed every week. Bioactivity of these materials was assessed at 7 days and 28 days time interval. Each specimen was sterilized under ultraviolet light for 20 min.

### 2.2. SEM analysis

Then the samples were air dried completely and were coated with gold (10 nm). They were observed under a scanning electron microscope connected to a secondary electron detector for energy dispersive X-ray analysis (EDX; Central instrumentation Facility, Manipal, Karnataka) at 5000x magnification.

## 3. Results

SEM analysis of group 1 revealed a compact and agglomerate lath-like appearance with uniform particle size. The surface shows presence of capillary channels across the mass of MTA plus after 28 days which are depicted by arrows in Fig. 2.

The EDX analysis showed a higher calcium deposition i.e., 95.76 wt % with small amount of phosphorous (4 wt%) after 7 days as shown in Fig. 1. After 28 days, chloride ions and oxygen were also visible. The wt % of phosphorous increased slightly whereas calcium wt % decreased to 44 % as shown in Fig. 2.

SEM analysis of group 2 reveals acicular and lath-like appearance of the precipitate on the material surface. Capillary channels were noted after 7 days which are depicted using arrows (Fig. 3). However, no channels were noted in SEM after 28 days due to presence of a thick precipitate of apatite on the material surface (Fig. 4). The amount of precipitate gradually increased from day 7 to day 28 and became more compact. Petal-like precipitate was also observed as shown using arrows in Fig. 4.

The EDX analysis showed 34 wt% calcium with other elements like oxygen, silica, aluminium, sodium and negligible amounts of phosphorous (Fig. 3). After 28 days, there was an increase in both calcium and phosphorous concentration (93 wt% and 6 wt% respectively). Silica, aluminium, bismuth became undetectable after 28 days as shown in Fig. 4.

## 4. Discussion

The chemical characteristics of dental materials in close contact with periapical tissues are predictive factors of their physical, chemical and biological properties (Borges et al., 2014). Tissue mineralization occurs when cells come in contact with these dental materials. The cells need to get attached to the surface of the material for the mineralization to occur. This surface morphology can be studied in vitro by immersing the biomaterials in a phosphate containing medium (Pedano et al., 2018; Yu et al., 2005). The amount of precipitate on the surface of biomaterials can be attributed to their bioactivity. The calcium released from the surface creates an alkaline pH which in turn is required for formation of hydroxyapatite (Gandolfi et al., 2010; Gandolfi et al., 2015; Gandolfi et al., 2013).

This phenomenon of apatite formation can be better visualized under SEM. SEM provides detailed high-resolution images of any sample by inducing a focused electron beam across the surface and detecting secondary or back scattered electron signal. An Energy Dispersive X-Ray Analyzer (EDX or EDA) is also used to provide elemental identification and quantitative compositional information of the sample. Each element produces its own characteristic set of X-ray lines at precisely defined energies. The measurement of these line energies indicates what elements are present (Borges et al., 2014). Hence, in this study, the surface morphology was studied using SEM and EDX which gives the qualitative and semi-quantitative composition of the surface of the material.

This study clearly demonstrated the apatite forming ability of both MTA Plus and the experimental group (MTA Plus with Chitosan). Both the groups showed a uniform deposition of calcium phosphate precipitates which differed in their morphology.

MTA Plus group showed a compact and agglomerate lath-like appearance with uniform particle size. The surface shows presence of capillary channels across the mass of MTA plus after 28 days which are depicted by arrows in Fig. 2. MTA Plus consists of an anhydrous phase that dissolves and forms a crystallized phase upon maturation. This crystallization can be seen as formation of different types of crystals on the surface of this biomaterial as also shown by other studies (Parirokh et al., 2018; Asgary et al., 2006; Fridland and Rosado, 2003). Upon immersion in phosphate containing medium, the crystal morphology changes from cubic crystals to either compact agglomerate (lath-like), petal-like or spherical with needle like appearance (acicular) (Lee et al., 2004; Reyes-Carmona et al., 2009). The occurrence of acicular crystallites is the first step of conversion of amorphous calcium phosphate to apatite (octa calcium phosphate and hydroxyapatite). These crystals are responsible for exchange of elements between them and the surrounding medium, resulting in morphologic alterations (Dorozhkin, 2009; Meyer and Eanes, 1978). The compact, lath-like crystals are related to maturation of the amorphous calcium phosphate into crystallized apatite (Meyer and Eanes, 1978; Weng et al., 1997). Group 1 (MTA Plus) showed the formation of matured crystals (lath-like) at 7 days and showed no change in crystal morphology even after 28 days. Similar studies have been performed previously on MTA and glass ceramics which showed formation of lath-like crystals on its surface after immersing the material in different types of medium (Lee et al., 2004; Reyes-Carmona et al., 2009; Weng et al., 1997; Tay et al., 2007).

Group 1 also revealed the formation of capillary channels on its surface after 28 days (Fig. 2). The presence of capillary structure, observed with SEM, could be an important cause of this material's porosity which can lead to micro-leakage (Fridland and Rosado, 2003). However, the formation of precipitate on the material will eventually fill these channels with apatite crystals (Bozeman et al., 2006). In this case, the amount of precipitate formed is not sufficient to fill the channels which will eventually lead to dissolution of material and micro-leakage. This study revealed the formation of a calcium compound (Wollastonite) on the surface of these calcium silicate materials under SEM-EDX. Wollastonite is a calcium-silica-oxygen compound which shows high bioactivity in vitro by forming hydroxyapatite crystals when immersed



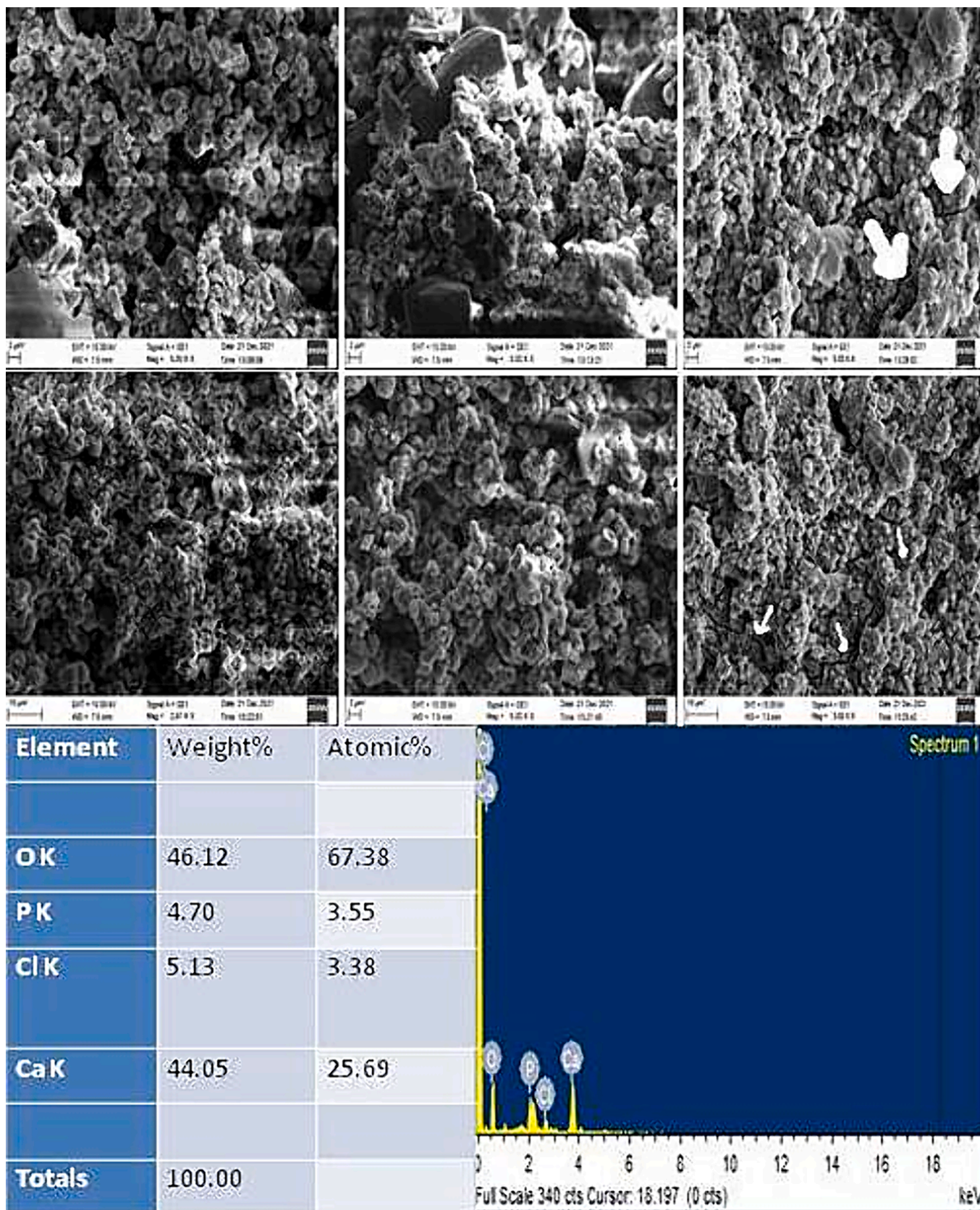


Fig. 2. SEM image and EDX analysis of Group 1 after 28 days.



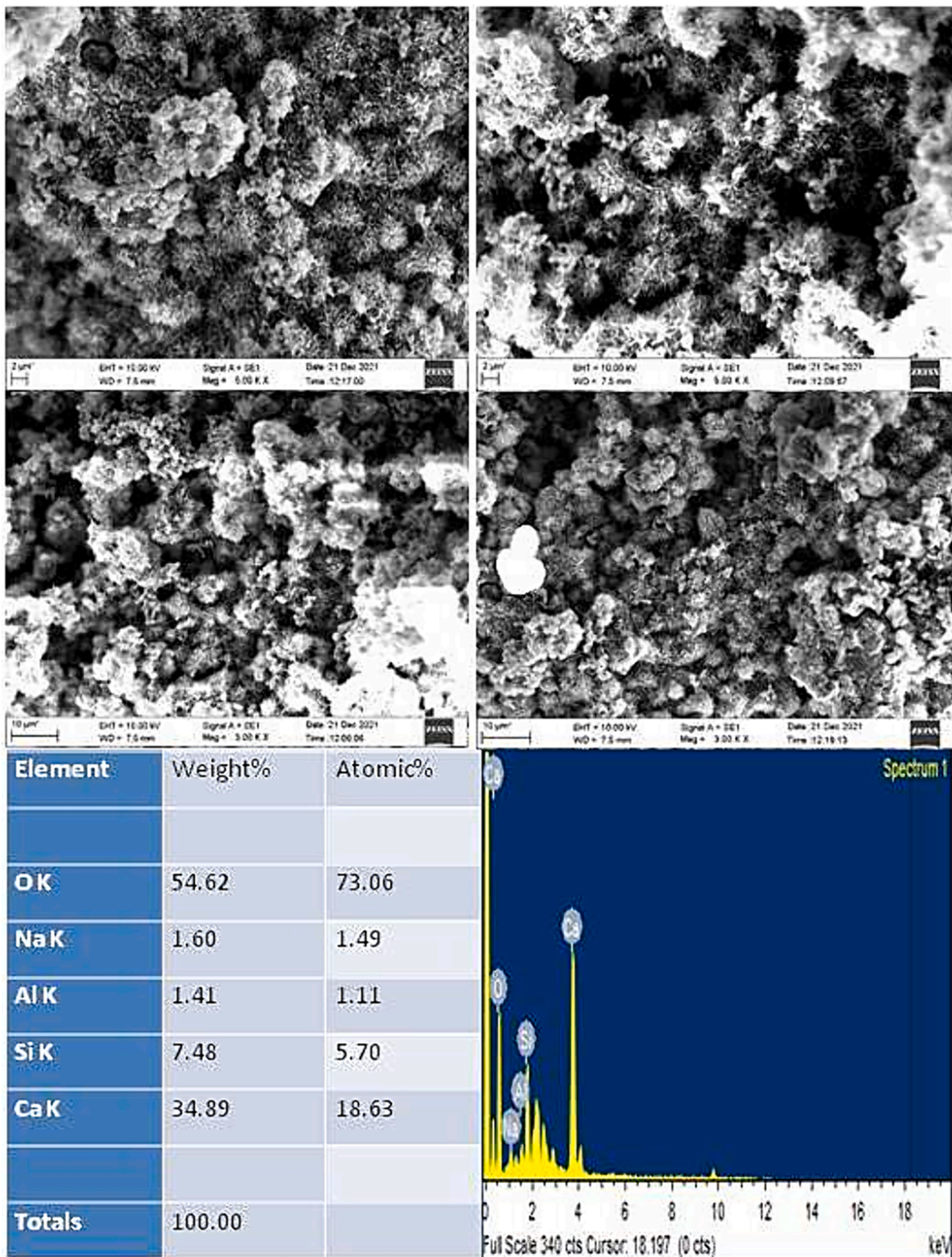


Fig. 3. SEM image and EDX analysis of Group 2 after 7 days.

in PBS. The ion (calcium) release from Wollastonite may affect the pH on the surface of the sample and creates the required alkaline environment. Another reason for the promoted bioactivity may relate to the Si-OH groups from the Wollastonite crystals which gives a negative charge to the compound surface. The negative charged surface attracts the

positively charged calcium ions from the PBS solution, forming calcium compounds like calcium silicate. The positively charged compound attracts the phosphate ions in return. After the apatite nucleation, the apatite continues to grow in the PBS solution due the alkaline environment (Chen et al., 2016).



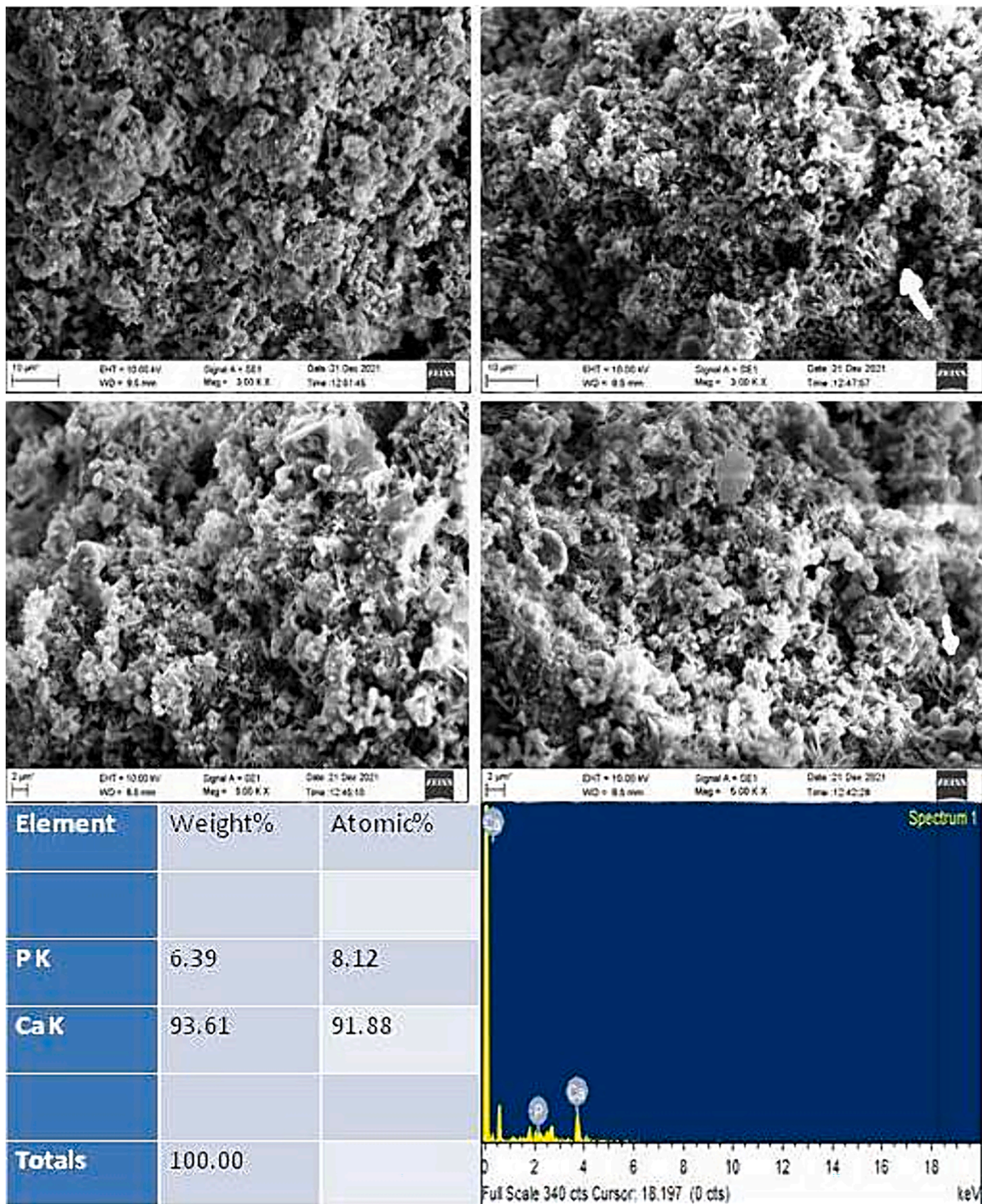


Fig. 4. SEM image and EDX analysis of Group 2 after 28 days.

The results of SEM can be related to the analysis of the composition obtained by EDX. There was a higher calcium deposition i.e., 95.76 wt% with small amount of phosphorous (4 wt%) after 7 days as shown in Fig. 1. The increase of calcium after 7 days is due to the ability of MTA Plus to form apatite crystals faster as explained previously under SEM analysis. The formation of oxygen and negligible amount of silica confirms the formation of Wollastonite compound. After 28 days, chloride ions and oxygen were also visible as shown in Fig. 2. The wt % of phosphorous was increased slightly whereas calcium wt % was

decreased to 44 %.

Similar study by Gandolfi in 2014 revealed that the levels of calcium and phosphate for MTA Plus were decreased after 28 days of immersion in PBS. This can be explained by the fact that there was precipitation of the Ca/P crystals on the surface of the samples (Gandolfi et al., 2015).

Group 1 released less amount of calcium after 28 days (Fig. 2) which may be insufficient to neutralize the acidic environment caused during pulpal inflammation. Also, studies have revealed that acidic surroundings make MTA less cohesive and more porous which may lead to micro-



leakage (Lee et al., 2004; Han et al., 2010; Neelakantan et al., 2019; Han and Okiji, 2013).

SEM analysis of group 2 reveals acicular and lathe-like appearance of the precipitate on the material surface. Capillary channels were noted after 7 days which are depicted using arrows (Fig. 3). However, no channels were noted on the surface after 28 days due to the presence of a thick precipitate on the material surface. The amount of precipitate gradually increased from day 7 to day 28 and became more compact.

This study initially showed formation of acicular crystals for group 2 (MTA Plus- Chitosan) which gradually changed to compact agglomerate lathe-like structures after 28 days indicating the formation of crystallized apatite (Figs. 3, 4). Few petal-like crystals were also observed as shown in Fig. 4. Petal-like crystals are related to formation of octa calcium phosphate, which is a transient phase seen during mineralization (Reyes-Carmona et al., 2009; Dorozhkin, 2009). The presence of these crystals confirms the bioactivity of both the materials. However, group 2 showed a slower rate of bioactivity (28 days to complete mineralization) as compared to group 1.

The EDX analysis of group 2 showed the release of more amount of calcium (Fig. 4) after 28 days. This creates the necessary alkaline environment to counteract the low pH along with formation of Wollastonite compounds. Increased amount of this compound is directly related to formation of increased apatite and thus increased bioactivity (Weng et al., 1997; Chen et al., 2016). Nonetheless, minor differences in the expected chemical composition reported in EDX/EDS analyses can be produced as a result of variances between the equipment used and the measurements carried out.

For group 2, the channels were noted after 7 days (Fig. 3). However, none could be seen after 28 days (Fig. 4) indicating that the amount of precipitate formation increased eventually and was sufficient to crystallize the channels. This confirms that the amount of precipitate containing apatite increased for group 2 after 28 days.

EDX analysis of group 2 showed that there was 34 wt% calcium at 7 days with negligible amount of phosphorous as shown in Fig. 3. After 28 days, there was an increase in both calcium and phosphorous concentration (93 wt% and 6 wt% respectively) as shown in Fig. 4. This can be explained by the fact that phosphorylated chitosan (P-chi) has a strong affinity to bind to calcium ions and hence induces calcium phosphate formation (<https://hdl.handle.net/1807/96284>). Other elements included oxygen, silica, aluminium, sodium, chlorine after 7 days (Wollastonite compound). Silica, aluminium, bismuth became undetectable after 28 days. Aluminium acts as a reactor in the calcium silicate cements whereas bismuth is used as a radio-opacifier and affects the precipitation of calcium hydroxide in the hydrated paste (Siboni et al., 2017; Camilleri, 2008).

## 5. Conclusion

Within the limitations of the present study, it was concluded that Chitosan can be used as a vehicle with MTA plus as the conjugate, since it has a greater potential to form apatite crystals on its surface. According to this study,

1. MTA Plus showed lathe-like apatite crystals and capillary channels at 7 and 28 days
2. MTA Plus-Chitosan conjugate showed acicular, lathe-like and petal shaped apatite crystals and a greater apatite forming ability after 28 days.

The limitations of the study were.

1. Though the SEM images show thick apatite layer formation on surface of biomaterials, apatite thickness was not measured using SEM.
2. Individual apatite crystal morphology was not visualized under SEM

## Declaration of competing interest

The authors declare that they have no known competing financial interests or personal relationships that could have appeared to influence the work reported in this paper.

## References

- Ahmadi, F., Oveysi, Z., Samani, S.M., Amoozgar, Z., 2015. Chitosan based hydrogels: characteristics and pharmaceutical applications. *Res Pharm Sci.* 10 (1), 1–16.
- Asgary, S., Parirokh, M., Eghbal, M.J., Stowe, S., Brink, F., 2006. A qualitative X-ray analysis of white and grey mineral trioxide aggregate using compositional imaging. *J Mater Sci Mater Med.* 17 (2), 187–191.
- Borges, Álvaro Henrique, et al., 2014. Analysis of Chemical Elements and Heavy Metals in MTA Fillapex and AH Plus. *OHDM* 13 (4), 1007–1012.
- Bozeman, T.B., Lemon, R.R., Eleazer, P.D., 2006. Elemental analysis of crystal precipitate from grey and white MTA. *J Endod.* 32 (5), 425–428.
- Camilleri, J., 2008. Characterization of hydration products of mineral trioxide aggregate. *Int Endod J.* 41 (5), 408–417.
- Chen, S., Cai, Y., Engqvist, H., Xia, W., 2016. Enhanced bioactivity of glass ionomer cement by incorporating calcium silicates. *Biomater.* 6 (1), e1123842.
- Dorozhkin, S.V., 2009. Calcium orthophosphates in nature. *Biology and Medicine. Materials (Basel)* 2 (2), 399–498.
- Fenice, M., Gorrasi, S., 2021. Advances in chitin and chitosan science. *Molecules* 26 (6), 1805.
- Fridland, M., Rosado, R., 2003. Mineral trioxide aggregate (MTA) solubility and porosity with different water-to-powder ratios. *J Endod.* 29 (12), 814–817.
- Gandolfi, M.G., Taddei, P., Tinti, A., Prati, C., 2010. Apatite-forming ability (bioactivity) of ProRoot MTA. *Int Endod J.* 43 (10), 917–929.
- Gandolfi, M.G., Siboni, F., Polimeni, A., Bossù, M., Riccitiello, F., Rengo, S., Prati, C., 2013. *In Vitro* screening of the apatite-forming ability, biointeractivity and physical properties of a tricalcium silicate material for endodontics and restorative dentistry. *Dent. J.* 1, 41–60.
- Gandolfi, M.G., Siboni, F., Botero, T., Bossù, M., Riccitiello, F., Prati, C., 2015. Calcium silicate and calcium hydroxide materials for pulp capping: biointeractivity, porosity, solubility and bioactivity of current formulations. *J Appl Biomater Funct Mater.* 13 (1), 43–60.
- Gurucharan, I., Saravana Karthikeyan, B., Mahalaxmi, S., Baskar, K., Rajkumar, G., Dhivya, V., Kishen, A., Sankaranarayanan, S., Gurucharan, N., 2023. Characterization of nano-hydroxyapatite incorporated carboxymethyl chitosan composite on human dental pulp stem cells. *Int Endod J.* 56 (4), 486–501.
- Han, L., Okiji, T., Okawa, S., 2010. Morphological and chemical analysis of different precipitates on mineral trioxide aggregate immersed in different fluids. *Dent Mater J.* 29 (5), 512–517.
- Han, L., Okiji, T., 2013. Bioactivity evaluation of three calcium silicate-based endodontic materials. *Int Endod J.* 46 (9), 808–814.
- Hiremath G, V Shyam Kumar, Yeli M. (2020) Biophysical Characterization of MTA Plus and Chitosan Conjugate for Biomedical Applications. 4(2): 6-10.
- Hiremath, G., Kulkarni, Singh M., Bhusan, P., Rajeev, N., Balam, N., 2020b. Antibiofilm efficacy of root-end filling materials against enterococcus faecalis - an in vitro study. *Endodontology* 32 (2), 86–90. <http://www.epj-conferences.org> or <https://doi.org/10.1051/epjconf/20122900034>.
- Lee, Y.L., Lee, B.S., Lin, F.H., Yun Lin, A., Lan, W.H., Lin, C.P., 2004. Effects of physiological environments on the hydration behavior of mineral trioxide aggregate. *Biomaterials* 25 (5), 787–793.
- Meyer, J.L., Eanes, E.D., 1978. A thermodynamic analysis of the amorphous to crystalline calcium phosphate transformation. *Calcif Tissue Res.* 25 (1), 59–68.
- Neelakantan, P., Berger, T., Primus, C., Shemesh, H., Wesselink, P.R., 2019. Acidic and alkaline chemicals' influence on a tricalcium silicate-based dental biomaterial. *J Biomed Mater Res B Appl Biomater.* 107 (2), 377–387.
- Parirokh, M., Torabinejad, M., Dummer, P.M.H., 2018. Mineral trioxide aggregate and other bioactive endodontic cements: an updated overview - part I: vital pulp therapy. *Int Endod J.* 51 (2), 177–205.
- Pedano, M.S., Li, X., Li, S., Sun, Z., Cokic, S.M., Putzeys, E., Yoshihara, K., Yoshida, Y., Chen, Z., Van Landuyt, K., Van Meerbeek, B., 2018. Freshly-mixed and setting calcium-silicate cements stimulate human dental pulp cells. *Dent Mater.* 34 (5), 797–808.
- Primozic, J., Hren, M., Mezeg, U., Legat, A., 2022. Tribocorrosion susceptibility and mechanical characteristics of as-received and long-term in-vivo aged nickel-titanium and stainless-steel archwires. *Materials (Basel).* 15 (4), 1427.
- Reyes-Carmona, J.F., Felipe, M.S., Philippe, W.T., 2009. Biomineralization ability and interaction of mineral trioxide aggregate and white portland cement with dentin in a phosphate-containing fluid. *J Endod.* 35 (5), 731–736.
- Ruan, Q., Moradian-Oldak, J., 2015. amelogenin and enamel biomimetics. *J Mater Chem b.* 3, 3112–3129.
- Siboni, F., Taddei, P., Prati, C., Gandolfi, M.G., 2017. Properties of Neo MTA Plus and MTA Plus cements for endodontics. *Int Endod J.* 50, e83–e94.
- Singh, M., Hiremath, G., Bhat, K.G., et al., 2020. Evaluation and Comparison of the Effect of MTA, MTA Plus, chitosan, and their conjugates on cell viability of human periodontal ligament fibroblasts: an *In Vitro* study. *J Oper Dent Endod* 5 (2), 74–78.
- Tay, F.R., Pashley, D.H., Rueggeberg, F.A., Loushine, R.J., Weller, R.N., 2007. Calcium phosphate phase transformation produced by the interaction of the portland cement component of white mineral trioxide aggregate with a phosphate-containing fluid. *J Endod.* 33 (11), 1347–1351.

- Tiskaya, M., Shahid, S., Gillam, D., Hill, R., 2021. The use of bioactive glass (BAG) in dental composites: a critical review. *Dent Mater.* 37 (2), 296–310.
- Tu, M.G., Ho, C.C., Hsu, T.T., Huang, T.H., Lin, M.J., Shie, M.Y., 2018. Mineral trioxide aggregate with mussel-inspired surface nanolayers for stimulating odontogenic differentiation of dental pulp cells. *J Endod.* 44 (6), 963–970.
- Vallittu, P.K., Boccaccini, A.R., Hupa, L., Watts, D.C., 2018. Bioactive dental materials- Do they exist and what does bioactivity mean? *Dent Mater.* 34 (5), 693–694.
- Walsh, R.M., He, J., Schweitzer, J., Opperman, L.A., Woodmansey, K.F., 2018. Bioactive endodontic materials for everyday use: a review. *Gen Dent.* 66 (3), 48–51.
- Weng, J., Liu, Q., Wolke, J.G., Zhang, X., de Groot, K., 1997. Formation and characteristics of the apatite layer on plasma-sprayed hydroxyapatite coatings in simulated body fluid. *Biomaterials* 18 (15), 1027–1035.
- Yu, S., Hariram, K.P., Kumar, R., Cheang, P., Aik, K.K., 2005. In vitro apatite formation and its growth kinetics on hydroxyapatite/polyetheretherketone http biocomposites. *Biomaterials* 26 (15), 2343–2352.